Artificial-Neural-Network-Based Sensorless Nonlinear Control of Induction Motors

Miroslaw Wlas, Zbigniew Krzemiński, Jarosław Guziński, Haithem Abu-Rub, *Member, IEEE*, and Hamid A. Toliyat, *Senior Member, IEEE*

***Abstract*—In this paper, two architectures of artificial neural networks (ANNs) are developed and used to correct the performance of sensorless nonlinear control of induction motor systems. Feedforward multilayer perception, an Elman recurrent ANN, and a two-layer feedforward ANN is used in the control process. The method is based on the use of ANN to get an appropriate correction for improving the estimated speed. Simulation and experimental results were carried out for the proposed control system. An induction motor fed by voltage source inverter was used in the experimental system. A digital signal processor and field-programmable gate arrays were used to implement the control algorithm.**

***Index Terms*—Artificial neural networks (ANNs), digital signal processor (DSP), field-programmable gate arrays (FPGAs), induction motor, nonlinear control, observer system, sensorless control.**

I. Introduction

THE application of artificial neural networks (ANNs) attracts the attention of many scientists from all over the world [1]. The reason for this trend is the many advantages which the architectures of ANN have over traditional algorithmic methods. Among the advantages of ANN are the ease of training and generalization, simple architecture, possibility of approximating nonlinear functions, insensitivity to the distortion of the network, and inexact input data. The use of ANN is practical at present that technological progress is rapid and the practical utilization of the system that mimics nature is possible.

ANNs can be used to identify and control nonlinear dynamic systems because they can approximate a wide range of nonlinear functions to any desired degree of accuracy. Moreover, they can be implemented in parallel and, therefore, shorter computational time. Also, they have immunity from harmonic ripples and have fault-tolerant capability.

Since the 1990s, several investigations into the applications of neural networks in the field of electrical machines and power electronics have appeared [2].

Manuscript received February 2, 2004; revised March 29, 2004. Paper no. TEC-00022-2004.

M. Wlas, Z. Krzemiński, and J. Guziński are with the Faculty of Electrical and Control Engineering, Gdańsk University of Technology, Gdańsk 80-952, Poland (e-mail: mwlas@pg.gda.pl).

H. Abu-Rub is with the Department of Electrical Engineering, Birzeit University, Birzeit, Palestine (e-mail: haithem@birzeit.edu).

H. A. Toliyat is with the Department of Electrical Engineering, Texas A&M University, College Station, TX 77843-3128 USA (e-mail: Toliyat@ee.tamu.edu).

Digital Object Identifier 10.1109/TEC.2005.847984

In recent years, many papers have appeared which deal with the use of ANN in modulation systems [3], [19], in breakdown detection [4], in control [5]–[7], in the estimation of state variables [8], [9], and in the identification of induction motor parameters [20].

In many papers [5], [10]–[15], the use of ANN has been tried for estimating the rotor angular speed. Among the methods used, it is possible to note two types of ANN designs. One is based on the machine model [10], and the other one uses stator currents and voltages for direct speed estimation [12], [13]. The input values to the neural speed observer presented in [12], [13] are the actual currents and voltages or their values from previous steps together with the magnitude of the stator current.

Several ANN architectures were implemented by the authors in simulations and in experiments for a 1.1-kW induction motor. Only two architectures are discussed in this paper due to their easy implementation on the digital signal processor (DSP) and short execution time for the sensorless induction motor drive.

In the proposed solution, the neural networks are used to correct the estimated rotor speed in the nonlinear control of induction motors [15], [21], [22]. The internal signals of the speed observer system were used to correct the observer's errors at steady states and during transients. The developed control system based on the speed observer is stable and robust.

II. Mathematical Model and Nonlinear Control of a Squirrel-Cage Induction Motor

The mathematical model of a squirrel-cage induction motor expressed in terms of the stator currents and rotor flux vector components in the stationary coordinate system are as follows:

$$\frac{di_{sx}}{d\tau} = a_1 i_{sx} + a_2 \psi_{rx} + a_3 \omega_r \psi_{ry} + a_4 u_{sx} \tag{1}$$

$$\frac{di_{sy}}{d\tau} = a_1 i_{sy} + a_2 \psi_{ry} - a_3 \omega_r \psi_{rx} + a_4 u_{sy} \tag{2}$$

$$\frac{d\psi_{rx}}{d\tau} = a_5 \psi_{rx} - \omega_r \psi_{ry} + a_6 i_{sx} \tag{3}$$

$$\frac{d\psi_{ry}}{d\tau} = a_5 \psi_{ry} + \omega_r \psi_{rx} + a_6 i_{sy} \tag{4}$$

$$\frac{d\omega_r}{d\tau} = \frac{L_m}{L_r J}(\psi_{rx} i_{sy} - \psi_{ry} i_{sx}) - \frac{1}{J} m_o \tag{5}$$

where u_{sx}, u_{sy}, i_{sx}, i_{sy}, ψ_{rx}, and ψ_{ry} are the stator voltages, stator currents, and rotor flux vectors components in the stationary xy coordinate system, ω_r is the angular speed of the

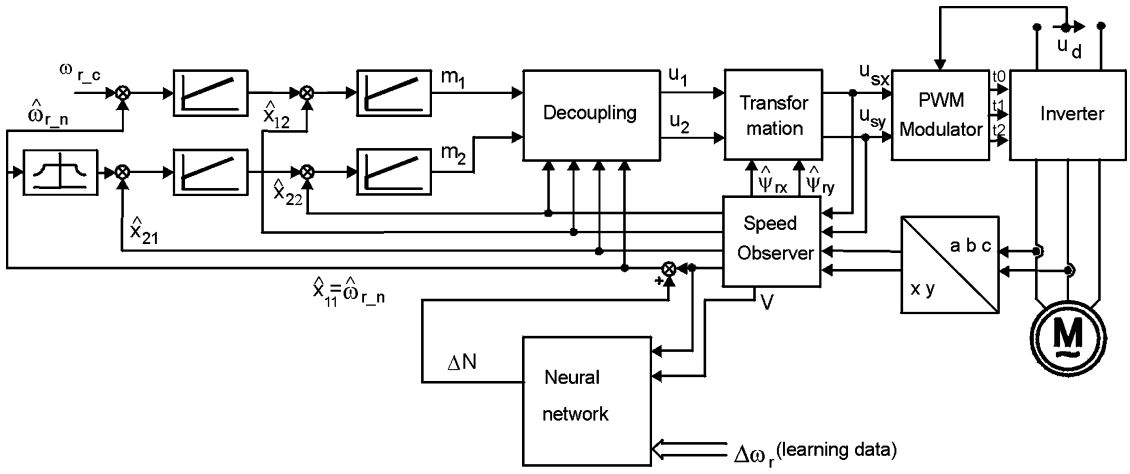

Fig. 1. Control system for the induction motor with speed observer and ANN corrector.

rotor shaft, L_m is the mutual inductance, J is the moment of inertia, m_0 is the load torque, and furthermore

$$
\begin{aligned}
a_1 &= -\frac{\left(R_s L_r^2 + R_r L_m^2\right)}{(L_r w_\sigma)} \\
a_2 &= \frac{(R_r L_m)}{(L_r w_\sigma)} \\
a_3 &= \frac{L_m}{w_\sigma} \\
a_4 &= \frac{L_r}{w_\sigma} \\
a_5 &= -\frac{R_r}{L_r} \\
a_6 &= \frac{R_r L_m}{L_r}
\end{aligned}
$$

where $w_\sigma = L_r L_s - L_m^2$, R_s, R_r, L_s, L_r, and L_m are the rotor and stator resistances and inductances, respectively, and τ is the time in per unit.

III. Nonlinear Linearization of Induction Motor Fed by Voltage-Source Inverters (VSIs)

In the case of using induction motor model fed by a pulsewidth-modulated (PWM) voltage-source inverter (VSI), the control signals are the voltage vector components.

Four novel state variables have been proposed for describing the motor model [15], [21]. The multiscalar variables may be interpreted as the rotor angular speed, scalar and vector products of the stator current and rotor flux linkages vectors, and the square of the rotor flux linkages represented in an arbitrary coordinate system xy as follows:

$$x_{11} = \omega_r \tag{6}$$

$$x_{12} = \psi_{rx} i_{sy} - \psi_{ry} i_{sx} = \psi_r i_s \sin(\delta) \tag{7}$$

$$x_{21} = \psi_{rx}^2 + \psi_{ry}^2 \tag{8}$$

$$x_{22} = \psi_{rx} i_{sx} + \psi_{ry} i_{sy} = \psi_r i_s \cos(\delta). \tag{9}$$

After taking into account the differential equations of new state variables, the following model is obtained:

$$\frac{dx_{11}}{d\tau} = \frac{L_m}{J L_r} x_{12} - \frac{1}{J} m_o \tag{10}$$

$$\frac{dx_{12}}{d\tau} = -\frac{1}{T_v} x_{12} - x_{11}\left(x_{22} + \frac{L_m}{w_\delta} x_{21}\right) + \frac{L_r}{w_\delta} u_1 \tag{11}$$

$$\frac{dx_{21}}{d\tau} = -2\frac{R_r}{L_r} x_{21} + 2R_r \frac{L_m}{L_r} x_{22} \tag{12}$$

$$\frac{dx_{22}}{d\tau} = -\frac{x_{22}}{T_v} + x_{11} x_{12} + \frac{R_r L_m}{L_r w_\delta} x_{21} + R_r \frac{L_m}{L_r} \frac{x_{12}^2 + x_{22}^2}{x_{21}} + \frac{L_r}{w_\delta} u_2 \tag{13}$$

where $T_\nu = w_\delta (R_r L_s + R_s L_r)$ and

$$u_1 = \psi_{rx} u_{sy} - \psi_{ry} u_{sx} \tag{14}$$

$$u_2 = \psi_{rx} u_{sx} + \psi_{ry} u_{sy}. \tag{15}$$

The compensation of nonlinearities present in (11) and (13) using the nonlinear feedback technique previously discussed leads to defining the new input variables m_1 and m_2 as

$$u_1 = \frac{w_\delta}{L_r}\left[x_{11}\left(x_{22} + \frac{L_m}{w_\delta} x_{21}\right) + m_1\right] \tag{16}$$

$$u_1 = \frac{w_\delta}{L_r}\left(-x_{11} x_{12} - \frac{R_r L_m}{L_r w_\delta} x_{21} - \frac{R_r L_m}{L_r} \frac{x_{12}^2 + x_{22}^2}{x_{21}} + m_2\right). \tag{17}$$

The sensorless nonlinear control system of induction motors with the speed observer system and ANN corrector described in the following sections and partially designed on the basis of previous equations is presented in Fig. 1.

IV. Rotor Speed Observer System

A new speed observer system has been proposed for the first time in [16]. The differential equations of the speed observer modified in this paper are as follows:

$$\frac{d\hat{i}_{sx}}{dt} = a_1\hat{i}_{sx} + a_2\hat{\psi}_{rx} + a_3\omega_r\hat{\psi}_{ry} + a_4 u_{sx} + k_3\left(k_1(i_{sx} - \hat{i}_{sx}) - \hat{\omega}_r\zeta_x\right) \tag{18}$$

$$\frac{d\hat{i}_{sy}}{dt} = a_1\hat{i}_{sy} + a_2\hat{\psi}_{ry} - a_3\omega_r\hat{\psi}_{rx} + a_4 u_{sy} + k_3\left(k_1(i_{sy} - \hat{i}_{sy}) - \hat{\omega}_r\zeta_y\right) \tag{19}$$

$$\frac{d\hat{\psi}_{rx}}{d\tau} = a_5\hat{i}_{sx} + a_6\hat{\psi}_{rx} - \zeta_y - k_2(\hat{\omega}_r\hat{\psi}_{ry} - \zeta_y) \tag{20}$$

$$\frac{d\hat{\psi}_{ry}}{d\tau} = a_5\hat{i}_{sy} + a_6\hat{\psi}_{ry} + \zeta_x + k_2(\hat{\omega}_r\hat{\psi}_{rx} - \zeta_x) \tag{21}$$

$$\frac{d\zeta_x}{d\tau} = k_1(i_{sy} - \hat{i}_{sy}) \tag{22}$$

$$\frac{d\zeta_y}{d\tau} = -k_1(i_{sx} - \hat{i}_{sx}) \tag{23}$$

$$\hat{\omega}_r = S\left(\sqrt{\frac{\zeta_x^2 + \zeta_y^2}{\hat{\psi}_{rx}^2 + \hat{\psi}_{ry}^2}} + k_4(V - V_f)\right) \tag{24}$$

where $\hat{}$ denotes estimated variables; and k_1, k_2, k_3, and k_4 are the observer gains and S is the sign of speed. The values ζ_x and ζ_y are the components of disturbance vector and V is the control signal obtained through experiments and V_f is the filtered signal V.

V. Correction of Speed Observer Using ANN

The coefficients k_1 to k_4 in the speed observer system have small values. Therefore, the operation of the observer system is stable and maintains small transient errors. The values of the coefficients significantly affect the quality of the calculated speed during transients. In [17], it is shown that the coefficient k_2 may depend on the rotor speed

$$k_2 = a + b \cdot |\hat{\omega}_{rf}| \tag{25}$$

where a and b are constant coefficients and $\hat{\omega}_{rf}$ is the estimated and filtered rotor speed.

The simulation and experimental tests showed that it is necessary to choose different values of the coefficients for different speeds, torques, and transients to minimize speed estimation errors. Therefore, it seems advantageous to keep constant coefficients k_1, k_2, and k_3 at the same time using ANN instead of the expression $k_4(V - V_f)$. If the difference between the actual and the estimated speed is used for network learning as a base signal, then the expression (24) will have the following form:

$$\hat{\omega}_{r\_n} = S\left(\sqrt{\frac{\zeta_x^2 + \zeta_y^2}{\hat{\psi}_{rx}^2 + \hat{\psi}_{ry}^2}} + \Delta N\right) \tag{26}$$

where ΔN is the output of the ANN.

The speed observer may be used in different control systems for rotor flux and speed estimation. The testing of the speed observer system with ANN was primarily done on an open-loop system with the V/f scalar control method.

The test was done for two structures of ANN, multilayer feedforward and recurrent, and with fuzzy logic. As an input to the multilayer-percepton ANN (MLP), the estimated speed $\hat{\omega}_r$, the change of speed in time $d\hat{\omega}_r/d\tau$, and two other variables V and filtered value V_f were used. These two internal signals are defined as follows:

$$V = \hat{\psi}_{rx}\zeta_y - \hat{\psi}_{ry}\zeta_x \tag{27}$$

$$\frac{dV_f}{d\tau} = \frac{1}{T_1}(V - V_f). \tag{28}$$

In the case of speed estimation in an open-loop system, the estimated multiscalar variable $\hat{x}_{12}$ is used as an additional input signal.

The basic criterion for the selection of ANN is the ability of being tested on the microprocessor system. In this paper, the main trend was not only to minimize the inputs to the network but also to use a minimum number of layers and neurons in each layer. Because of the speed change detection in time, a signal $d\hat{\omega}_r/d\tau$ was calculated every ten sampling periods. It means that every 1.5 ms for the sampling period is equal to 150 μs (microseconds). At the same time, the calculation of ANN and the addition of the corrector from the network output ΔN were realized in each calculation step (every 150 μs).

For the correction of rotor speed, a computer simulation showed that it is sufficient to use double-layer ANN with a few neurons in the hidden layer and one in the output layer. The neurons in the hidden layer have sigmoid activation function (hyperbolic tangent), and the output neuron has a linear function. For the determination of the neurons number in the hidden layer of the feedforward network, an evolution programming method was used.

As a result of studying the ANN architecture and the initial weights, it is noted that for the feedforward multilayer network, it is enough to use two layers with one output neuron and four or five neurons in the hidden layer.

A. Training Process

Supervised neural networks applied to the speed observer were trained to produce the desired output correction to the estimated speed. Implementation of these supervised networks, feedforward and recurrent, was carried out in two steps. In the first step, four groups of 2500 input–output training data were obtained from simulation of the complete drive system. In the next step, the trained ANN was implemented in the experimental sensorless drive. For proper operation with high and low load, the neural networks had to be retrained in the system with speed measured by an encoder.

Determination of the ANN weight to correct the rotor speed is an iterative process, which consists of the following steps.

Step 1) First, data from the simulation and experiment are selected. In the case of the computer simulation of the drive system, four groups of training signals, each containing 2500 training pairs, for the open-loop system are selected. In the case of the experiment, the process was the same but

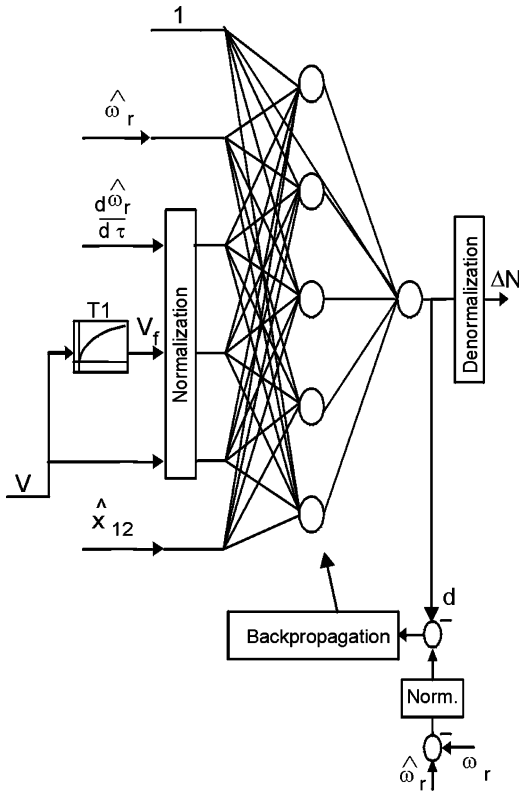

Fig. 2. MLP neural network for correction of estimated speed in an open-loop control system.

each group contained 500 learning pairs. Each pair consists of network inputs $\hat{\omega}_r$, $d\hat{\omega}_r/d\tau$, V, V_f, $\hat{x}_{12}$, and the desired output $\Delta\omega_r$. The network inputs V, V_f, $d\hat{\omega}_r/d\tau$ and the desired output $\Delta\omega_r$ were normalized.

Step 2) The architecture of the (5–5–1) feedforward MLP neural network is presented in Fig. 2. The network had been trained on the basis of the simulation and experimental data. The initial weights were determined using the evolution programming method.

Step 3) To improve the learning process, the input data to the ANN were the subject of polynomial interpolation.

Step 4) The training of MLP ANN was performed by the Luenberger–Marquardt (L–M) backpropagation algorithm in the first step and standard gradient descent with momentum backpropagation, and adaptive learning rate in the second step [10].

If Elman ANN is used, the testing procedure should be performed by the method described above.

Step 5) The procedure repeats the third step for the entire next learning data considering that each new learning starts from the weights, which were determined in the previous learning process.

Step 6) The last stage of checking the performance of the speed corrector was testing using data that are different than the learning ones. In both simulation and experimental cases, the reversal of the machine speed was checked. The simulation results are presented in Fig. 3 and the experimental results are presented in Fig. 4. The actual rotor speed is ω_r, and the estimated and corrected using ANN is $\omega_{r\ n}$.

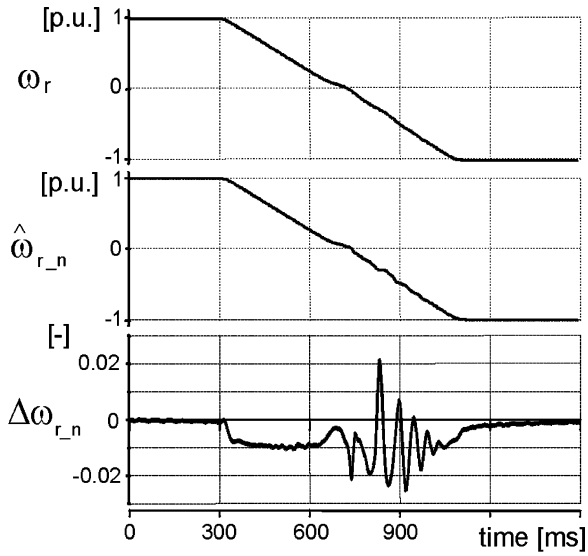

Fig. 3. Simulation waveforms during speed reversal (from 0.9 to −0.9 p.u.) for V/f control method and MLP (5-5-1) ANN.

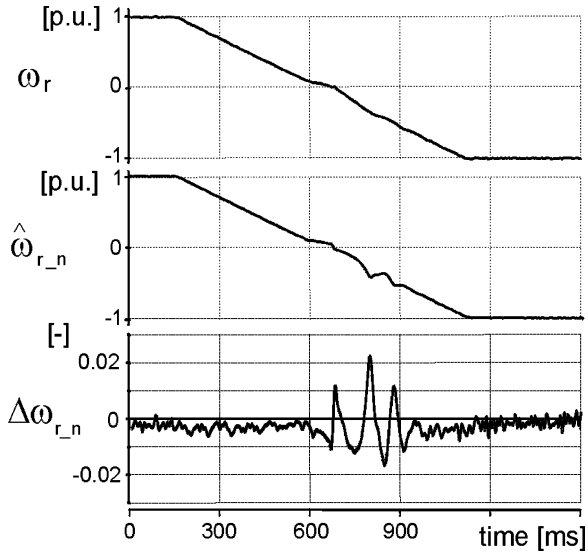

Fig. 4. Experimental waveforms during speed reversal (from 0.8 to −0.8 p.u.) for V/f control method and MLP (5-5-1) ANN.

Due to the use of an ANN speed corrector, the steady-state error was decreased nearly to zero. After nearly zeroing the error, small oscillations are observed. However, as a result of using the ANN corrector, it does not exceed 2.5%.

The same oscillations observed during the simulation test shown in Fig. 3 were also observed during the experiment depicted in Fig. 4. The experimental results prove the simulation findings.

B. ANN Speed Corrector in a Closed-Loop System

In the case of a closed-loop system, the structure of the MLP feedforward ANN could be simplified. The calculated variable

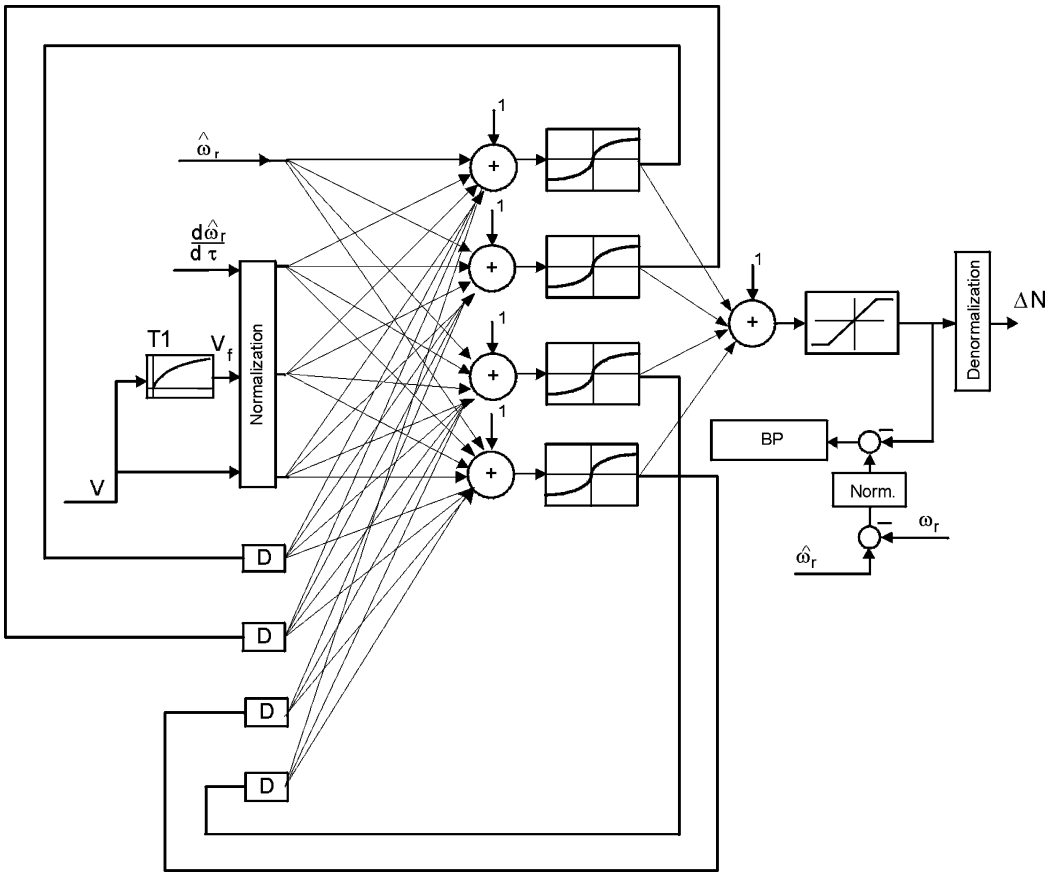

Fig. 5. Recurrent Elman neural network for correction of estimated rotor speed in a closed-loop control system.

x_{12} is not used. The simulation and experimental tests showed that the significant effect on the speed estimation error has the dynamic of the torque and not its value. The (5–5–1) architecture of MLP feedforward ANN is shown in Fig. 2. All neurons in the hidden and output layers have a bipolar sigmoid active function. Many learning rules were checked and it was concluded that the fastest that gives the least mean value is the L–M method.

In addition to the feedforward ANN, the recurrent ANN is used to correct the rotor speed. The architecture of the Elman recurrent ANN is presented in Fig. 5. This contains four neurons with sigmoid active function in the hidden layer and one output neuron with linear limited active function. In the case of using Elman networks, the recurrent loop is provided once again to all neurons in the hidden layer by a delay D. This makes it possible to detect and generate time-varying patterns in the Elman network. The stored values from the previous step are used in the current step in this ANN.

As a testing rule of the Elman network, a method with backpropagation error algorithm was used. For the recurrent network, the following training steps in each time period occurs.

Step 1) The entrance input sequence is provided to the network, and its output is calculated and compared with the target speed to generate an error.

Step 2) The error is backpropagated to find gradients of errors for each weight and bias. This gradient is actually an approximation since the contributions of weights and biases to the error, via the delay recurrent connection, are ignored. This approximate gradient is then used to update the weights with the standard gradient descent with momentum method. The waveforms of the two training methods are shown in Fig. 6. The errors are in per unit.

The parameters used to train the network are learning rate $\alpha = 0.01$ and error tolerance 0.1%. As in the case of the open-loop system, the training parameters were changed and the network was learned for different learning coefficients. The learning data are presented in Table I. Less learning error is obtained for the Elman network. The useful characteristics of the Elman network make it possible to decrease the average learning error to less than 0.01%, which is not possible when using the feedforward ANN.

C. Simulation Results of the Nonlinear Closed-Loop Control System With ANN Corrector

Properties of the presented system have been investigated using the simulation method. All results are presented in the per-unit system. The simulation was prepared using programs written in C language. The simulation results were used to describe the characteristics of the drive system with the speed observer and correction introduced with and without feedforward or recurrent ANN. The closed-loop control system was presented in Fig. 1.

The results of simulated rotor speed reversal are presented in Fig. 7. The variables calculated in the observer system are

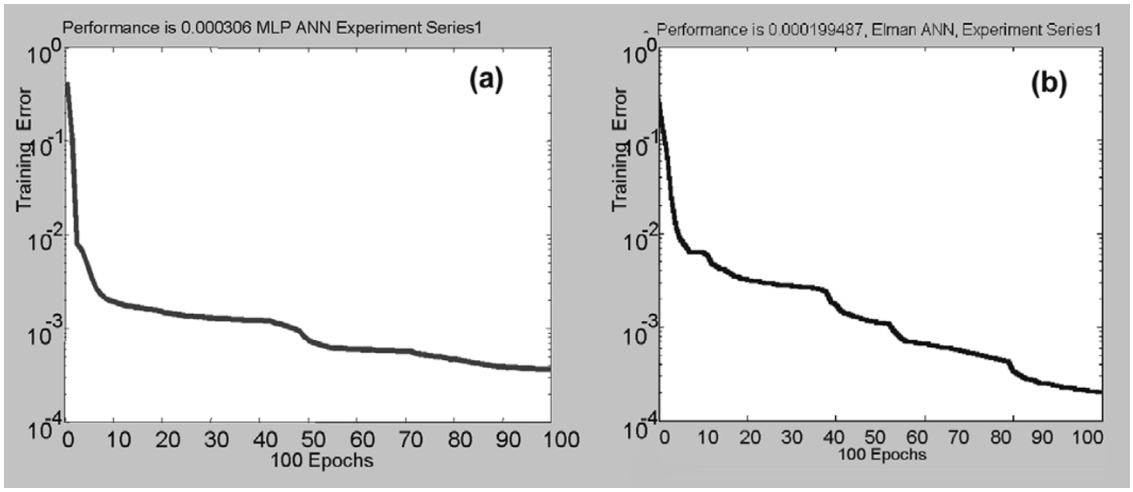

Fig. 6. L–M training method of feedforward ANN. (a) Error backpropagation of Elman ANN. (b) Based on the experimental data.

TABLE I
PARAMETERS OF THE IMPLEMENTED NEURAL NETWORKS

Parameters	Value
Number of training pairs – from simulation	4x2500
Number of training pairs – from experiment	4x500
Training coefficient	0.02
Tolerated estimation error	10^{-4}
The tolerated error difference in the next 100 training cycles	10^{-6}

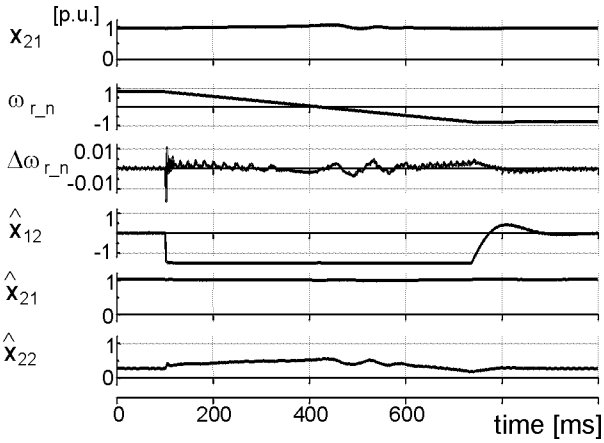

Fig. 7. Transients during motor speed reversal for system with MLP ANN (4–5–1) speed corrector.

noted with $\hat{}$. The error of estimated speed $\Delta\omega_{r\,n}$ does not exceed 0.5% except for a short period during which fast torque changing occurred. After zero crossing, oscillations with small magnitude appear in the waveforms of variables $\hat{x}_{21}$, $\hat{x}_{22}$, and in the error of the estimated speed. The oscillation does not affect the values of the torque and speed. The results during zero speed are presented in Fig. 8. The system maintains stability and operates correctly at zero speed when the motor is loaded. The observed torque oscillation denotes the speed oscillation close

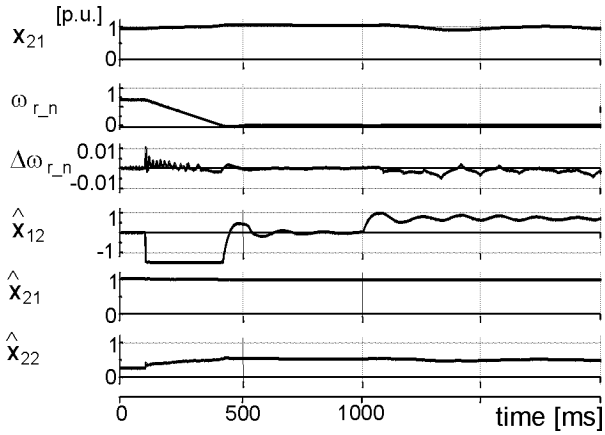

Fig. 8. Transients during zero speed with MLP ANN (4-5-1) speed corrector.

to zero speed. This is caused by the necessity to detect a speed sign in the observer system.

The network effect on the waveforms that are similar to the testing data was checked by changing the controller's parameters and keeping the observer coefficients constant.

Speed estimation in the closed-loop system for big parameters of speed and torque controllers when the feedforward ANN is applied is shown in Fig. 9. The correction of the observer system using ANN is very essential for small speeds. The correction value ΔN is nearly zero for high speed. This is proof that the observer system estimates the rotor speed correctly at high speed. During the transient, the speed error does not exceed 2%.

The operation of the Elman recurrent ANN while decreasing the gains of speed, torque, and electromagnetic (EM) controllers is presented in Fig. 10. The error of speed correction does not exceed 1% of the rated speed. Limitation of the dynamic in the control system corrects the characteristics of the speed observer and ANN corrector.

VI. EXPERIMENTAL RESULTS OF THE NONLINEAR CLOSED-LOOP CONTROL SYSTEM WITH ANN CORRECTOR

In practical implementation of electrical drives, an interesting solution is to use a specialized microcontroller in the control

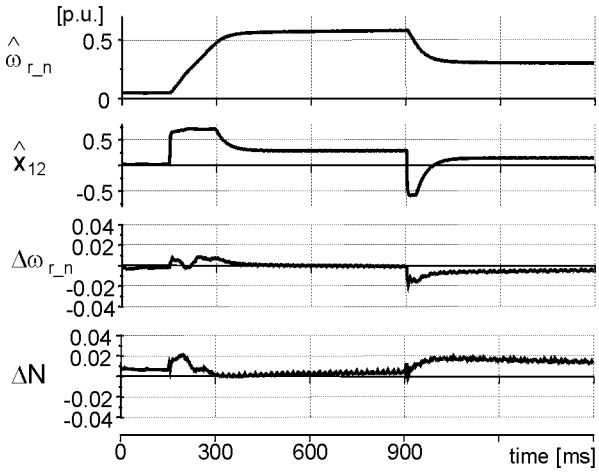

Fig. 9. Simulation results during the speed variations: $\omega_{\mathrm{r\_command}} = 0.05$; 0.6; 0.3 p.u.; (ANN MLP 4-5-1).

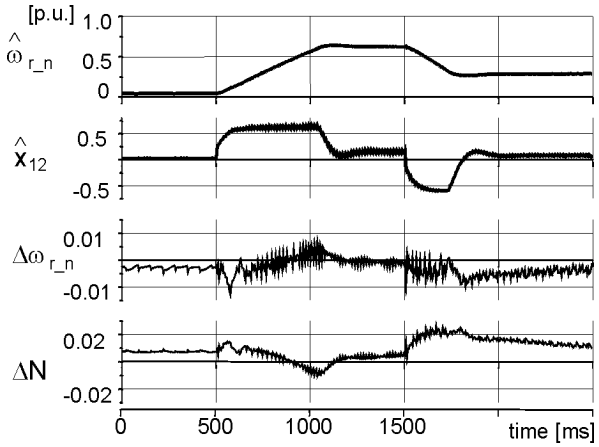

Fig. 10. Results of speed estimation with correction based on the use of recurrent Elman (4-4-1) ANN in the nonlinear closed-loop system during speed variations $\omega_{\mathrm{r\_command}} = 0.05$; 0.7; 0.3 p.u.

board. Such circuits are equipped with all indispensable interfaces. They allow for reducing costs and size of the control board. Smaller size of the digital circuits also decreases the sensitivity to external disturbances.

The experimental setup consists of the following elements:

- machine unit, squirrel cage induction motor-dc generator;
- voltage inverter;
- input/output (I/O) board with analog-to-digital converter and field-programmable gate-array (FPGA) system;
- signal processor board ADSP21065L;
- PC computer with programming for commanding parameters and viewing waveforms;
- the central element of the drive is a control system. It consists of a SH1 v. 1 board with DSP ADSP21065L. The SH1 board is programmed to work as an individual controller. It can be connected to an IBM PC via the serial interface RS232.

The characteristics of the nonlinear control system of induction motors with a speed observer and ANN corrector were experimentally tested using the 1.1-kW induction motor used in the simulations. The error of real speed estimation using the observer system may be somewhat different from the simulation

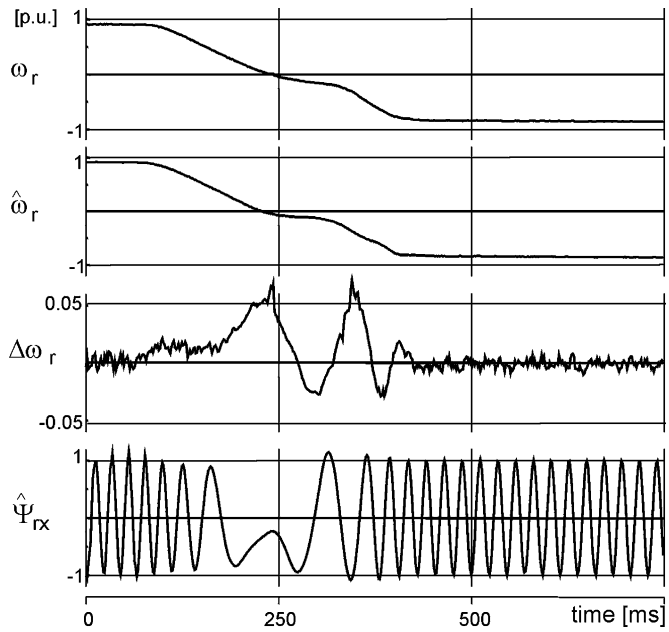

Fig. 11. Experimental results for speed reversal without ANN.

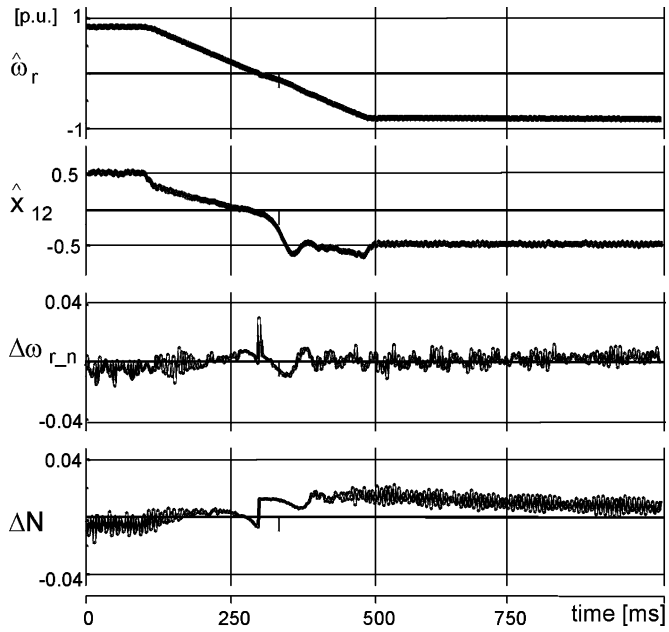

Fig. 12. Experimental results of speed reversal for the control system with speed correction when using Elman (4-4-1) ANN, the sampling period is Timp=100 μs.

results shown in Figs. 11–14. This results from the measurement error, which is added to the estimation error because of the speed reversal in the system without ANN. The speed calculated using (26) is plotted in Fig. 11. The error during speed reversal is caused by the measurement error and is about 5% during transient around zero and is about 1% at the steady-state.

Speed reversal when using the (4–4–1) architecture of the Elman network is shown in Fig. 12. Again, the effect of the measurement error is seen when speed is crossing zero but the transient error does not exceed 2%. Such a small error not only results from the proper action of the ANN corrector but also from more frequent correction and more exact voltage generation because of reducing the sampling period to 100 μs. The decrease

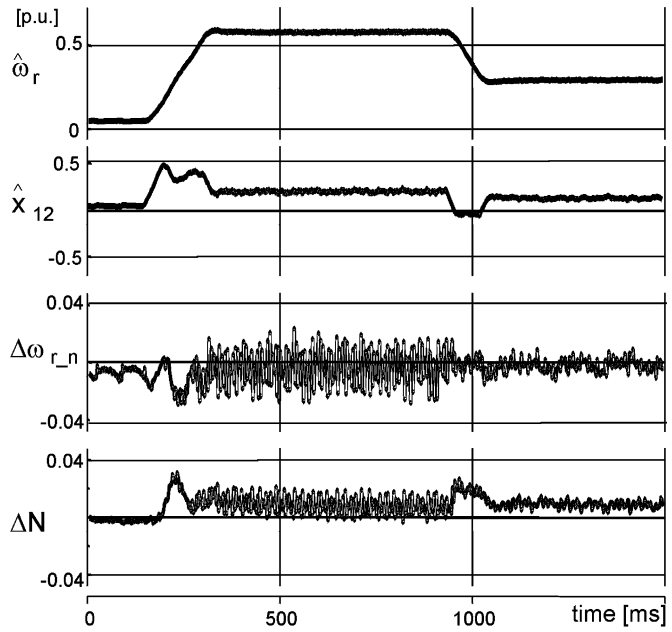

Fig. 13. Experimental results by using MLP feedforward ANN during speed variations $\omega_{\mathrm{r\_command}} = 0.05$; 0.6; 0.3 p.u. (MLP 4-5-1); Timp $=150\ \mu$s.

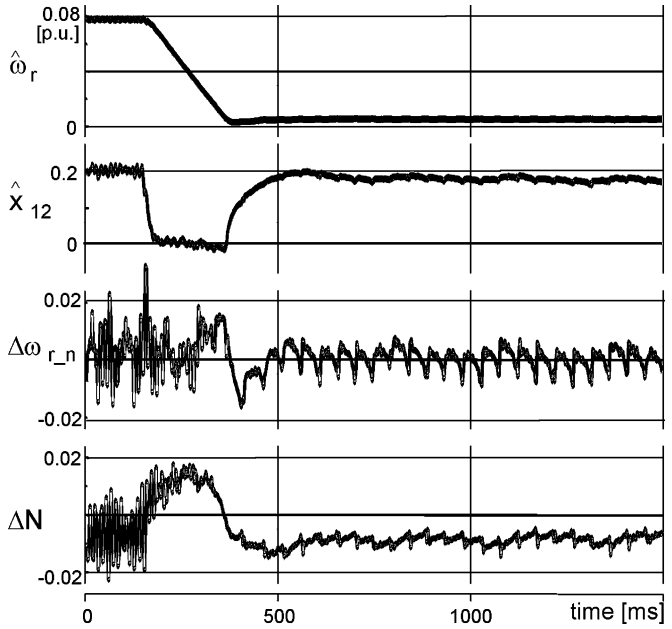

Fig. 14. Experimental results for braking under load when using Elman ANN: $\omega_{\mathrm{r\_command}} = 0.8$; 0.03 p.u.

of the sampling period below such value in a closed-loop system is not possible because the actual time of the closed-loop system is equal to 88.4 μs.

The experimental results obtained when using the (4–5–1) structure of the MLP feedforward ANN are presented in Fig. 13. The network was trained using four set of data from simulations, and four from experiments. The error between the measured speed and the estimated and corrected speed $\Delta\omega_{\mathrm{r\_n}}$ does not exceed 2% at the steady-state and during the transients.

In the next experiment, the breaking mode of the motor was checked and attempts were made to keep nearly zero speed operation while applying active load on the shaft. The speed variations from 0.8 to 0.03 p.u. is shown in Fig. 14. The speed estimation error $\Delta\omega_{r\_n}$ oscillates around zero and does not exceed 1% of the rated speed in the steady-state. The situation in transient is not much worse. The speed corrector is based on the (4–4–1) structure of the Elman network, which properly corrects the estimated speed in both steady-state and transients.

Comparative tests of the speed observer operation with and without the ANN corrector were conducted. This was done to check the correctness of our proposal of using the ANN corrector instead of conventional constant coefficients in the speed observer. Different operating points were checked. As a criterion, the integral of the square error between the actual and estimated speed has been chosen. The results of five different speeds are shown in Table II.

TABLE II
INTEGRALS OF SQUARE ERROR FOR DIFFERENT ROTOR SPEED

Rotor angular speed in [p.u.]	Error E when using standard correction	Error E when using Elman network
0.1	0.005871	0.002065
0.2	0.008662	0.002468
0.5	0.003913	0.002654
0.7	0.005215	0.003744
0.8	0.007668	0.005153

VII. CONCLUSION

In this paper, two ANN architectures were developed to enhance the performance of sensorless control of the induction motor in two ways.

A significant correction of speed estimation is provided especially during transients. The estimation error was significantly reduced. The load changes almost do not affect the speed estimation process. The speed is correctly estimated at zero speed and the whole control system operates well near standstill although the motor is loaded.

Because of using the Elman recurrent ANN or a two-layer feedforward ANN, the speed estimation errors during transients are reduced from 5% to 3% while at the steady-states are from 1% to 0.5% in experimental tests. The ANN was trained offline to correct the performance of the speed observer system.

ACKNOWLEDGMENT

The authors would like to thank the help of D. O'Toole from Cony High School, Augusta, ME, in preparing the final manuscript.

REFERENCES

[1] J. M. Zurada, *Introduction to Artificial Neural Systems*. St. Paul, MN: West, 1992.
[2] B. K. Bose, "Expert system, fuzzy logic and neural network application in power electronics and motion control," *Proc. IEEE*, vol. 82, no. 8, pp. 1303–1323, Aug. 1994.
[3] M. Kaźmierkowski and D. Sobczuk, "Investigation of neural network current regulator for VS-PWM inverters," in *Proc. 1994 Int. Conf. Power Electronics Motion Control*, Warsaw, Poland, pp. 1009–1014.
[4] B. Raison, F. Francois, G. Rostaing, and J. Rogon, "Induction drive monitoring by neural networks," in *Proc. IEEE Int. Conf. Industrial Electronics, Control Instrumentation*, Nagoya, Japan, 2000, pp. 859–863.

[5] G. Henneberger and B. Otto, "Neural network application to the control of electrical drives," in *Proc. Conf. Power Electronics Intelligent Motion*, Nuremberg, Germany, 1995, pp. 103–123.
[6] Y. S. Kung, C. M. Liaw, and M. S. Ouyang, "Adaptive speed control for induction motor drive using neural network," *IEEE Trans. Ind. Electron.*, vol. 42, no. 1, pp. 9–16, Feb. 1995.
[7] G. Kulawski and M. Bryś, "Stable adaptive control with recurrent networks," in *J. Int. Federation Automatic Control Automatica*, Jan. 2000, vol. 36, pp. 5–22.
[8] M. G. Simoes and B. K. Bose, "Neural network based estimation of feedback signals for a vector controlled induction motor drive," *IEEE Trans. Ind. Appl.*, vol. 31, no. 3, pp. 620–629, May/Jun. 1995.
[9] T. Orłowska-Kowalska and C. T. Kowalski, "Neural network based flux observer for the induction motor drive," in *Proc. Int. Conf. Power Electronics Motion Control*, Budapest, Hungary, 1996, pp. 187–191.
[10] L. Ben-Brahim and R. Kurosawa, "Identification of induction motor speed using neural networks," in *Proc. Power Conversion Conf.-Yokohama*, Yokohama, Japan, 1993, pp. 689–694.
[11] D. Sobczuk, "Application of ANN for control of PWM inverter fed induction motor drives," Ph.D. thesis, Tech. Univ. Warsaw, Inst. Control Ind. Electron., Warsaw, Poland, 1999.
[12] T. Orłowska-Kowalska and M. Pawlak, "Implementation of neural network speed estimator with help of TMS320C31 DSP," in *Proc. Int. Conf. Electrical Drives Power Electronics*, The High Tataras, Slovakia, Oct. 5–7, 1999, pp. 292–297.
[13] T. Orłowska-Kowalska and P. Migas, "Influence of neural network structure on the induction motor speed estimation quality," in *Proc. Int. Conf. Electrical Drives Power Electronics*, The High Tataras, Slovakia, Oct. 5–7, 1999, pp. 23–31.
[14] P. Vas, *Sensorless Vector and Direct Torque Control*. London, U.K.: Oxford Univ. Press, 1998.
[15] Z. Krzemiński, "Speed and rotor resistance estimation in observer system of induction motor," in *Proc. 4th Eur. Conf. Power Electronics*, Florence, Italy, 1991, pp. 583–589.
[16] ——, "A new speed observer for control system of induction motor," in *Proc. IEEE Int. Conf. Power Electronics Drive Systems*, Hong Kong, 1999, pp. 555–560.
[17] Z. Krzemiński and M. Włas, "Neural network based tuning of speed observer for control system of induction motor," in *Proc. 10th Int. Conf. Power Electronics Motion Control*, Dubrovnik & Cavtat, Croatia, Sep. 9–11, 2002, pp. 1–10.
[18] Z. Jovankovic, M. Zalman, and I. Belai, "Neural network estimation of rotor speed for direct field oriented control," in *Proc. 9th Int. Conf. Power Electronics Motion Control*, vol. 6, Kosice, Slovakia, 2000, pp. 47–51.
[19] P. Brandstetter and M. Skotnica, "Control of the VSI-PWM inverter using artificial neural network," in *Proc. Int. Conf. Electrical Drives Power Electronics*, The High Tataras, Slovakia, 1999, pp. 80–83.
[20] D. Balara and J. Timko, "Identification of induction motor parameters with use of neural networks taking into account main flux saturation effect," in *Proc. 9th Int. Conf. Power Electronics Motion Control*, vol. 6, Kosice, Slovakia, 2000, pp. 17–23.
[21] H. Abu-Rub, J. Guzinski, Z. Krzeminski, and H. Toliyat, "Speed observer system for advanced sensorless control of induction motor," *IEEE Trans. Energy Convers.*, vol. 18, no. 2, pp. 219–224, Jun. 2003.
[22] J. Guzinski, H. Abu-Rub, and H. A. Toliyat, "An advanced low-cost sensorless induction motor drive," *IEEE Trans. Ind. Appl.*, vol. 39, no. 6, pp. 1757–1764, Nov./Dec. 2003.
[23] H. Abu-Rub, J. Guzinski, Z. Krzeminski, and H. Toliyat, "Advanced control of induction motor based on load angle estimation," *IEEE Trans. Ind. Electron.*, vol. 51, no. 1, pp. 4–14, Feb. 2004.

Miroslaw Wlas was born in Ostróda, Poland. He received the M.S. degree in electrical engineering and the Ph.D. degree from the Technical University of Gdańsk, Gdańsk, Poland, in 1996 and 2003, respectively.

His research interests include neural-network applications to sensorless machine control. He is working on the implementation of real-time control systems.

Zbigniew Krzemiński received the Ph.D. degree from the Technical University of Lódź, Lódź, Poland, in 1983, and the D.Sc. degree from Silesian Technical University, Gliwice, Poland, in 1991.

Currently, he is a Professor with the Gdańsk University of Technology, Gdańsk, Poland. His main areas of research are modeling and simulation of electric machines, control of electric drives, and digital-signal-processor (DSP) systems.

Jarosław Guziński received the M.Sc. and Ph.D. degrees in electrical engineering from the Technical University of Gdańsk, Gdańsk, Poland, in 1994 and 2000, respectively.

Currently, he is an Adjunct with the Faculty of Electrical and Control Engineering, Gdańsk University of Technology, Gdańsk, Poland. His current interests include sensorless control of electrical motors, digital signal processors (DSPs), electric cars and remote control, and data acquisitions using computer nets.

Haithem Abu-Rub (M'99) received the Ph.D. degree in electrical engineering from the Technical University of Gdańsk, Gdańsk, Poland, in 1995.

Currently, he is an Associate Professor with Birzeit University, Birzeit, Palestine. His main research interests include electric motor drives, power electronics, and electrical machines.

Hamid A. Toliyat (S'87–M'91–SM'96) received the B.S. degree in electrical engineering from the Sharif University of Technology, Tehran, Iran, in 1982, the M.S. degree in electrical engineering from West Virginia University, Morgantown, in 1986, and the Ph.D. degree in electrical engineering from the University of Wisconsin–Madison, in 1991.

Currently, he is a Professor in the Department of Electrical Engineering, Texas A&M University, College Station. He has published many technical papers and has received one U.S. patent with several pending. His main research interests and experience include multiphase variable speed drives for traction and propulsion applications, fault diagnosis of electric machinery, analysis and design of electrical machines, and sensorless variable speed drives.

Dr. Toliyat is a member of Sigma Xi. He is the Vice Chairman of IEEE-IAS Electric Machine Committee and serves on several IEEE committees and subcommittees. He is an Editor of the IEEE TRANSACTIONS ON ENERGY CONVERSION, and an Associate Editor of the IEEE TRANSACTIONS ON POWER ELECTRONICS. He is a member of the Editorial Board of *Electric Machines and Power Systems Journal*. He received the Texas A&M Select Young Investigator Award in 1999, the Eugene Webb Faculty Fellow Award in 2000, the Space Act Award by NASA in 1999, and the Schlumberger Foundation Technical Awards in 2000 and 2001, and the 1996 IEEE Power Engineering Society Prize Paper Award.